TECHNICAL NOTE
D-48

GROUND MEASUREMENTS OF THE SHOCK-WAVE NOISE FROM

AIRPLANES IN LEVEL FLIGHT AT MACH NUMBERS

TO 1.4 AND AT ALTITUDES TO 45,000 FEET

By Domenic J. Maglieri, Harvey H. Hubbard,
and Donald L. Lansing

Langley Research Center
Langley Field, Va.

NATIONAL AERONAUTICS AND SPACE ADMINISTRATION

WASHINGTON   September 1959

NATIONAL AERONAUTICS AND SPACE ADM

TECHNICAL NOTE D-48

GROUND MEASUREMENTS OF THE SHOCK-WAVE NOISE FROM

AIRPLANES IN LEVEL FLIGHT AT MACH NUMBERS

TO 1.4 AND AT ALTITUDES TO 45,000 FEET

By Domenic J. Maglieri, Harvey H. Hubbard,
and Donald L. Lansing

SUMMARY

Time histories of noise pressures near ground level were measured
during flight tests of fighter-type airplanes over fairly flat, partly
wooded terrain in the Mach number range between 1.13 and 1.4 and at
altitudes from 25,000 to 45,000 feet. Atmospheric soundings and radar-
tracking studies were made for correlation with the measured noise data.

The measured and calculated values of the pressure rise across the
shock wave were generally in good agreement. There is a tendency for
the theory to overestimate the pressure at locations remote from the
track and to underestimate the pressures for conditions of high tailwind
at altitude. The measured values of ground-reflection factor averaged
about 1.8 for the surfaces tested as compared to a theoretical value
of 2.0. Two booms were measured in all cases. The observers also gener-
ally reported two booms; although, in some cases, only one boom was
reported. The shock-wave noise associated with some of the flight tests
was judged to be objectionable by ground observers, and in one case the
cracking of a plate-glass store window was correlated in time with the
passage of the airplane at an altitude of 25,000 feet.

INTRODUCTION

During flight at supersonic speeds, shock waves are formed which may
extend to the ground and cause objectionable noise. The passage of these
shock waves past an observer results in rapid changes in the atmospheric
pressure which are interpreted by the ear as explosive-type sounds,
commonly referred to as sonic booms. These sonic-boom phenomena were
first reported during the maneuvers of military airplanes, and more
recently, with the advent of more powerful airplanes, they have been
observed for steady flight conditions. This shock-wave noise may become
a particularly serious problem for any sustained flight operations at
supersonic speeds.

The phenomena of shock-wave propagation in a homogeneous atmosphere have been studied both experimentally and theoretically in reference 1. The phenomena of shock-wave generation from a body of revolution traveling in a homogeneous atmosphere are treated theoretically in reference 2. The work of reference 3 expands the theory of reference 2 in an attempt to account for nonhomogeneities in the atmosphere and presents a method of predicting the lateral extent of the area on the ground which would be exposed to the shock-wave noise pressures from an airplane in flight.

Some comprehensive measurements have been made of the shock-wave peak overpressures within 200 to 4,000 feet of fighter-type airplanes in flight (refs. 4 and 5). These measured shock-wave pressures were in good agreement with the calculated values by the method of reference 2. Wind-tunnel measurements of the shock-wave pressures from small bodies (ref. 6) varying in shape also have shown good agreement with the theory of reference 2.

Some data relating to the ground pressures from supersonic flight at high altitudes are given in references 4, 5, 7, and 8. Although some subjective observations were reported from steady flight conditions in reference 4, no measurements at ground level were reported. Ground pressures were measured in the work of reference 5 during shallow dives at low supersonic speeds and at altitudes up to 28,000 feet, and the results are summarized in reference 7. Very few measurements of the ground pressures resulting from steady level flight at high altitude are available except those of reference 8. These latter data are for fighter-type airplanes at Mach numbers up to 1.40 and at altitudes to 45,000 feet.

The present paper deals with the tests reported in reference 8 and includes more detailed analyses of the experimental data. In particular, time histories of ground pressures measured near the airplane track and at a lateral distance of several miles are presented. For some of these tests, both free-air- and reflected-pressure time histories are included. The results of atmospheric soundings and radar-tracking studies are correlated with the measured ground noise pressures. Also included are descriptions of the instrumentation and techniques used in the tests.

SYMBOLS

d equivalent body diameter, ft

K_1 ground-reflection factor

K_2 airplane body-shape factor

$$k = \frac{1}{K_1 K_2 (M^2 - 1)^{1/8}(d/l)}$$

l airplane length, ft

M airplane Mach number

p_a ambient pressure at altitude, lb/sq ft

p_o ambient pressure at ground level, lb/sq ft

Δp_f pressure rise across shock wave in free air, lb/sq ft

Δp_o pressure rise across shock wave at ground level, lb/sq ft

Δp_r pressure rise across reflected shock wave, lb/sq ft

Δt time interval between bow wave and tail wave, sec

V airplane ground velocity, ft/sec

x distance between shock waves in horizontal plane, ft

y perpendicular distance from measuring station to flight path, ft

λ rise time (time for ambient pressure to rise to maximum peak overpressure value), sec

μ Mach angle, $\sin^{-1} \frac{1}{M}$

APPARATUS AND METHODS

Test Conditions

Time histories of the noise pressures near ground level were measured during high-altitude flights of fighter-type airplanes in the vicinity of the NASA Wallops Station. Data were obtained during straight and level flight at nearly constant Mach number. The altitude varied from 25,000 to 45,000 feet, the Mach number varied from 1.13 to 1.4, and the horizontal distance from the flight track at which data were recorded varied from about 2.0 to 14.0 miles.

A plan-view map of the test area is shown in figure 1. Superposed on this map are the tracks of the flights along with the location of the three ground measuring stations denoted A, B, and C. Station A was located about 300 yards from the shoreline, whereas stations B and C were located inland in farming areas near the junctions of secondary roads. In addition to obtaining measured noise pressures, the operators and observers at the three stations recorded their reactions to the booms and also, when possible, observed the visible reaction of other persons in the vicinity.

Atmospheric soundings and radar-tracking studies were made with the aid of equipment located at station A for correlation with the measured noise data. The terrain in the vicinity of the measuring stations is partly wooded and the elevation ranges from sea level to 60 feet.

Test Airplanes

Photographs of the test airplanes are shown as figure 2. Test airplane 1 (fig. 2(a)), which was used for flights 1 to 6 (see fig. 1), has a fuselage length of 67.4 feet and a weight of about 39,000 pounds. Test airplane 2 (fig. 2(b)), which was used for flight 7, is 47 feet in length and weighs 28,500 pounds.

Noise Measuring Instrumentation

Noise-pressure measurements were obtained with the aid of a commercially available condenser-type microphone and a resistance-type strain-gage pressure pickup. Photographs of these items of equipment are shown as figure 3. The microphone system has a usable frequency range from 5 to 10,000 cps and is flat within ±2 decibels within the range of 10 to 7,000 cps. This system was calibrated with the aid of a 400-cps sine wave at a pressure level of 121 decibels. The pressure-gage system has a flat frequency response from 0 to 100 cps and was calibrated with a static pressure. The signals from both instruments were recorded with the aid of an FM tape recorder having a flat frequency response from 0 to 2,000 cps. At least one microphone was located at each of the measuring stations, whereas pressure pickups were located only at stations A and B. For the first four flights, the measuring equipment at stations A, B, and C were in close proximity to the ground and in an open area. For the remaining three flights, only station A was operated, and the measuring equipment was oriented as shown in figure 4. One microphone and the pressure pickup were mounted in a plywood board to measure the ground pressures. Two other microphones were attached to a mast, one being 5 feet and the other 30 feet above ground level. These latter microphones detected the free-air pressure as well as the reflected component.

Radar Tracking

An attempt was made to obtain continuous radar tracks during the supersonic portion of all flights. Radar plan position and altitude data were plotted automatically at 1-second intervals. The actual plan position plots from the SCR-584 tracking radar for flights 2 to 6 are shown in figure 1. From these data and other related measurements taken during the test, airplane Mach number was calculated. Although radar plots were not obtained for flights 1 and 7, airplane altitude, heading, plan position, and Mach number were estimated from pilot observations. All flights were flown in such a manner as not to pass directly over the radar station so that continuous radar tracks could be obtained.

Atmospheric Soundings

Rawinsonde observations were taken within an hour of the flight time to establish the temperature, pressure, and wind characteristics of the atmosphere to altitudes of 50,000 feet. The temperature, pressure, and speed of sound obtained from these soundings for each flight are shown at various altitudes in figure 5 and are associated with the appropriate numbered flights. The standard ICAO atmospheric conditions (ref. 9) of pressure, temperature, and speed of sound are also shown in the figure for comparison. In addition to these measured quantities, wind velocity and direction have been calculated from radiosonde data for each of the soundings of figure 5. The wind velocity has been resolved into components parallel to and perpendicular to the airplane flight path and are shown in figure 6 at various altitudes.

RESULTS AND DISCUSSION

Time Histories of Noise Pressures

A summary of the measured ground-pressure data for all the flights obtained at the various stations is given in table I. Some selected time histories from which the data were obtained are reproduced in figures 7, 8, and 9 to illustrate some of the physical phenomena involved.

Presented in figures 7(a) and (b) are the time histories of the ground shock noise pressures from flight 1 as obtained, respectively, at measuring stations A and B. The top pressure trace in each case was obtained with the aid of the pressure pickup having a response limited to low frequencies. The bottom pressure trace in each case was obtained with the aid of a microphone system which was lacking in low-frequency response but had a much better high-frequency response. For all traces,

positive pressure increases are associated with an upward trace deflection. Time increases from left to right for all traces of the figure.

The top pressure trace of figure 7(a) provides a good indication of the sequence of events as the airplane shock waves sweep past a pressure sensing device on the ground. The first rapid pressure increase in the positive direction is due to the passage of the bow wave. Then follows a relatively slow decrease in pressure to negative values after which a second rapid compression occurs as the tail wave passes. Thus the pressure signature of the airplane is seen to be similar to the "N waves" generated by projectiles and reported in reference 1.

Measurements with a microphone, as in the lower trace of figure 7(a), differ from those of the pressure gage because of the differences in the frequency responses of the two systems. The microphone is better able to follow the rapid pressure changes associated with the shock fronts but does not reproduce the slowly varying pressures in between. The peak overpressures Δp_O and the period of the wave Δt, which are given in this paper, were all evaluated from microphone records, such as those of figure 7. The listed values of pressure rise apply directly to the bow wave since there was some difficulty associated with establishing the reference atmospheric pressure at the time of arrival of the tail-wave shock front.

The general characteristics of the time histories of ground noise pressure obtained at station B (fig. 7(b)) are generally similar in nature to those obtained at station A (fig. 7(a)). The values of the peak overpressures Δp_O are lower than those at station A and the rise time λ, which is the time it takes the ambient pressure to rise to peak overpressure Δp_O at the bow wave, is also longer as is the period of the wave Δt.

The differences in the pressure-trace characteristics at stations A and B cannot be explained in detail from the measurements taken at the time of the tests. The lateral distance from the airplane flight track to station A was about 3.7 miles, whereas the lateral distance to station B was about 10.5 miles. (See fig. 1.) Not only are the propagation distances different, but the propagation paths for the two cases differ and they have different elevation angles with respect to the ground. Before reaching station A, the waves travel mainly over water, whereas at station B the waves approach over land at a lesser angle of incidence. In this latter case, the atmospheric and terrain effects would probably be relatively more important.

Figure 8 includes the time histories of noise pressures from flights at four altitudes, as measured at station A. It can be noted that with the exception of flight 1 the values of pressure rise generally decrease

as altitude increases. There is, however, no consistent variation of Δt with altitude. There were differences in flight Mach number, lateral distance, reflection factor, and, in particular, in the atmospheric conditions, all of which would tend to account for these differences. Each of these pressure time histories exhibits a short rise time λ which was consistently observed at locations near the flight track.

Some indication of the manner in which the shock waves are reflected from the ground surface is given in figure 9. In this figure the pressure time histories were obtained at the ground level and at elevations of 5 feet and 30 feet using the test setup of figure 4. For the trace of figure 9(a), the free-air and reflected wave arrive at the microphone, which was flush mounted in a plywood board at ground level, at about the same time and tend to add directly. For the microphone locations above the ground surface (figs. 9(b) and 9(c)), the reflected wave arrives at some time interval after the incident wave, and the resulting pressure wave is double peaked. The trace of figure 9(c) is of particular interest because the pressures associated with the incident and reflected wave can be evaluated directly, and the ground-reflection factors can then be calculated. The reflection factor K_1 is defined as follows:

$$K_1 = \frac{\Delta p_f + \Delta p_r}{\Delta p_f} \tag{1}$$

where Δp_f is the pressure rise across the incident or free-air wave

and Δp_r is the pressure rise across the reflected wave. For a sandy ground surface and for a hard plywood surface, the values of the reflection factors calculated from the measured data averaged about 1.8.

Ray Paths

The manner in which winds and temperature affect the propagation of shock waves from high altitudes to the ground can be illustrated with the aid of ray-path diagrams. If there were no temperature or wind gradients in the atmosphere between the airplane and the ground, the shock waves generated by the airplane would extend to the ground in a straight line at an angle μ determined by the flight Mach number. This wave would then propagate perpendicular to itself at approximately the speed of sound, the rate of propagation depending on the amount of overpressure; the path along which any segment of the wave propagates is also a straight line extending to the ground.

The temperature and wind gradients present during the tests as noted in figures 5 and 6, respectively, caused the waves to propagate faster at

8

some altitudes than at others; thus, a bending of the ray paths resulted. The temperature lapse rate which existed during the tests resulted in a higher speed of propagation near the ground. This results in a beneficial bending upward of the ray path which limits the extent of the boom or causes it to miss the ground altogether. The wind may affect the wave propagation velocity in such a way as to either add to the effects of temperature or to oppose them.

In order to illustrate the relative rates of wave propagation at the various altitudes, the data of figure 5 for temperature and the data of figure 6 for winds have been combined in figure 10. In figure 10 are illustrated the wave propagation velocities at various altitudes for the various tests conducted. A method is outlined in reference 3 for the calculation of the radius of curvature of the ray path if a linear variation is assumed in the propagation velocity from the airplane to the ground. A straight line was faired through the data of figure 10 for the purpose of calculating the curvature of the ray paths by the method outlined in reference 3. The results of these calculations are included in figure 11 where the calculated ray paths for some sample cases of the present tests are shown, along with the calculated ray paths for a homogeneous atmosphere. In all cases, the horizontal scale is the distance along the ground, and the vertical scale is the slant distance measured from the observation point perpendicular to the flight path.

In flights 1, 3, and 4 of figures 11(a), 11(b), and 11(c), respectively, there was a headwind present (fig. 6) that had the effect of adding to the beneficial temperature effect by decreasing the radius of curvature of the ray path and hence increasing its length. Of particular interest is flight 4 (fig. 11(c)) where the temperature and wind effects were of such a magnitude as to cause the ray path to miss the ground completely.

In the case of flights 5 and 6 (figs. 11(d) and 11(e)), there was a strong tailwind present (fig. 6), the effects of which tended to cancel out the beneficial effects of the temperature gradient. This is indicated by the fact that the ray-path radius of curvature is considerably greater, thus resulting in a shorter ray-path length.

Comparison With Theory

Magnitude of pressure rise.- A method is available for estimating values of Δp_o for various operating conditions. A convenient form of this expression for engineering use is as follows:

$$\Delta p_o = K_1 K_2 \left(\frac{\sqrt{p_a p_o}}{y^{3/4}}\right)\left(M^2 - 1\right)^{1/8}\left(\frac{d}{l}\right)l^{3/4} \tag{2}$$

This equation, which is presented in reference 8, indicates that the pressure rise Δp_o depends upon the ground-reflection factor K_1, which may vary between 1.0 and 2.0; the equivalent body-shape factor of the airplane K_2, which may vary from approximately 0.55 to 0.8; the airplane altitude term, which involves both distance y and the pressure expression $\sqrt{p_a p_o}$; airplane Mach number M; airplane fineness ratio term $\frac{d}{l}$; and airplane length l. The quantity d is defined as the diameter of a circle having an area equivalent to the maximum cross-sectional area of the airplane in a plane perpendicular to its longitudinal axis.

For any given airplane the length, fineness ratio, and body-shape factor are fixed and the ground pressures are then a function of the ground-reflection factor, the airplane altitude, and airplane Mach number. Equation (2) does not account for other variables such as the wind direction and velocity, the temperature gradient, the airplane lift and deviation from steady level flight, and propagation losses in the atmosphere.

Some of the ground-pressure data measured during the present tests are plotted in figure 12 in a form convenient for comparison with calculations by equation (2). The ordinate of the figure is $k \dfrac{\Delta p_o}{\sqrt{p_a p_o}}$, where

$$k = \frac{1}{K_1 K_2 (M^2 - 1)^{1/8} \left(\frac{d}{l}\right)}$$ and the abscissa is distance in airplane lengths

y/l from the ground station perpendicular to the flight path. The factor k is introduced for the purpose of accounting for variations in airplane length, fineness ratio, Mach number, and so forth, so that all of the test conditions can be represented by one theoretical curve. For the calculations of airplane 1, it was assumed that $K_1 = 1.8$, $K_2 = 0.645$, $l = 67.4$ feet, and $d/l = 0.13$. Likewise for airplane 2, it was assumed that $K_1 = 1.8$, $K_2 = 0.645$, $l = 47$ feet, and $d/l = 0.138$.

The calculated values, based on the assumptions of no temperature gradient and zero wind, are seen to drop off rapidly as the distance y increases. This trend is also substantiated in general by the measurements, particularly those near the track of the airplane. It should be noted that the data points for flights 1 and 3 were taken under different atmospheric conditions than those of flights 5 and 6. Examination of atmospheric sounding data (figs. 5 and 6) for the circular and square data points (fig. 12) for flights 1 and 3 indicated that there were moderate headwinds of from 0 to 30 ft/sec prevailing at altitude. Atmospheric sounding data for the diamond and triangular data points for flights 5

and 6 indicated a very similar temperature gradient closely simulating that of a standard atmosphere but with tailwinds of from 60 to 100 ft/sec. The data measured near the track seem to fall into two groups, both of which show the same relative dropoff with altitude as the theory predicts, but fall to each side of the calculated curves for these widely varying atmospheric conditions. The solid data points of figure 12 represent measurements made at stations at least 10 miles off the track. These measured values are generally lower than those calculated by equation (2) which does not account for refraction effects due to temperature and wind gradients.

Some insight into the manner in which refraction affects the lateral extent of the area affected by the boom is given in figure 13 in which experimental data are given for airplane 1 at altitudes of 25,000 and 35,000 feet. Measured pressures obtained at the various measuring stations are shown as a function of lateral distance from the track in miles. The theoretical curves are calculated with the use of equation (2) for the airplane flight conditions of $M = 1.22$ and $M = 1.4$ and the value of K_1 assumed to be 1.8. The theoretical curves indicate a maximum pressure along the flight track in each case and a decreasing pressure with increasing lateral distance. The lateral locations of the sudden cutoffs due to refraction effects, as denoted by the vertical dashed lines, are taken from reference 3 and are for a standard ICAO atmosphere and for zero wind. The distance to the cutoff point may vary according to the wind velocity, wind-velocity gradient, and wind direction as suggested qualitatively in figure 11.

Refraction effects arise because the air near the ground level is at a higher temperature than the air at altitude; this resulted in a more rapid propagation of the wave near the ground. This difference in propagation results in a bending upward of the ray paths in such a manner that they may miss the ground completely at large distances from the track. For the lower altitude case, as illustrated in figure 13(a), the pressures near the track are relatively high and there is a rapid decrease in pressure amplitude with increased lateral distance. At the higher altitude (fig. 13(b)) the pressures on the track tend to be lower and the boom pressures are detectable at greater lateral distances. It is believed that the data points for the extreme distances of figure 13 are approximately the cutoff points because they were barely audible to the station operators.

Time intervals of bow and tail wave pressures.- In addition to the values of pressure rise, time intervals Δt were also determined from the records for each of the tests. The measured time intervals are given in table II along with values calculated from the following expression:

$$\frac{x}{l} = \frac{2.22M^2}{\left(M^2 - 1\right)^{3/8}} \left(\frac{d}{l}\right)\left(\frac{y}{l}\right)^{1/4} \tag{3}$$

where x is the distance between the front and the rear shock waves in a plane parallel to the flight path. From a knowledge of x the time intervals may be calculated as follows:

$$\Delta t = x/V$$

where V is the ground velocity of the airplane as listed in table II. Equation (3) is obtained from reference 2 and is also presented as equation 33.27 in reference 7 except for the constant. The constant of equation (3), which is a function of body shape, is given in references 5 and 7 as 1.82 for a parabolic body. This value differs from the value of 2.22 of the present paper and it is believed that this difference is due to an error in the evaluation of an integral in the original work (ref. 2).

It can be seen that the calculated values are, in most cases, higher than the measured values. The reasons for the discrepancies between the measurements and the calculations are not readily apparent. Equation (3) was derived for the condition of a homogeneous atmosphere. There is, thus, some question about the effects on the time interval of such parameters as the wind, pressure, and temperature gradients of a nonhomogeneous atmosphere. Some of the effects of the nonhomogeneous characteristics of the atmosphere are considered in reference 10. Equation (3) is recommended for only a rough prediction of the shock-wave separation distances.

Reactions and Observations of Observers

In addition to the ground measurements presented in table I, some reactions and comments of various observers were obtained for some cases where measurements of disturbances or booms were available, and these are presented in table III. The observers and operators at the measuring stations recorded the number of booms that they perceived during each test and made an evaluation of the intensity. Additional data were obtained from people having no prior knowledge of the tests who either called in by telephone on their own initiative or who were observed by the measuring-station operators.

For all flights where records were obtained, the measurements indicated two sharp pressure rises which would be sensed by observers as two booms if the time interval between booms was sufficient so that the human ear could discriminate between them. In general, two booms were reported but there was occasionally some difference of opinion among observers at the same station whether one or two booms were heard. The measured time intervals Δt are on the order of 1/8 second although the extreme variations for these tests were from 0.121 to 0.220 second. (See table III.) Hence there is some indication that 1/8 second is near the lower time interval limit for discrimination of two sounds of this nature.

The human reaction to the shock-wave noise was fairly well correlated with the nature of the pressure time history. In particular, it was found that for peak overpressures up to about 0.5 lb/sq ft at ground level, the observers did not consider the booms objectionable and likened them to distant thunder or explosions. Those people who were observed during the tests did not react unusually and seemed unaware of the disturbances, nor were any comments by phone received. For ground pressures of from 0.5 lb/sq ft to about 1.0 lb/sq ft, the observers considered the booms tolerable but, to some extent, bothersome. Again no unusual reactions were exhibited by workers observed in the vicinity. For ground pressures exceeding 1.0 lb/sq ft, the observers were startled even though fore-warned of the impending boom. Observers considered these booms objectionable and likened them to very close-range thunder.

As a matter of interest, all booms associated with the records of figure 8 were judged to be objectionable. It should be noted that the rise times of figure 8 are relatively short, and in each case the observers likened the associated booms to sharp claps of thunder. In general, the records obtained at locations remote from the track had longer rise times as indicated in figure 7(b). A longer rise time is an indication that the high-frequency content of the wave has diminished, probably due to atmospheric and terrain absorption. Of particular interest is a comparison of the records in figures 7(b) and 8(b) where there were marked differences in the rise times λ. Since the reactions of observers were much different, as indicated in table III (flight 1), there is a suggestion that rise time (wave shape) may be as important as the pressure magnitude with regard to observer reaction.

In addition to the ground observations, an attempt was made to observe the booms from another airplane. During some of the tests a two-engined high-wing propeller-driven airplane used for communications between measuring stations was located in the air in the test area at an altitude of about 2,000 feet with engines at reduced power. The pilot of this airplane commented that no booms were detectable possibly due to the presence of other noise from the reciprocating engines and propellers.

As expected, the pilot of the generating airplane was not aware of the disturbances he created since he moved along at the same speed as the disturbances.

Structural Damage

As indicated in table III, damage to a large plate-glass store window was reported during a flight at an altitude of 25,000 feet (flight 3). The nature of the damage incurred is shown by the schematic diagram of figure 14. The radar track of the airplane passed nearly over the building and the reported time of the damage correlated well with the

flight time. Although ground noise pressures were not measured at the site of the reported damage, they were estimated to be somewhat in excess of the 1.75 lb/sq ft measured at station A.

The radar track direction, the flight Mach number, and the orientation of the building were such that the shock front impinged nearly normal to the window surfaces. The damage shown by the insert indicates that the 128-inch by 90-inch center window panel, which was firmly supported only at the top and bottom, had a crack extending almost horizontally across its width. No glass pieces fell out nor was any damage noted to the two adjacent panels of glass. The pressures incurred in this test may be near the magnitude where damage might begin to occur for large commercially installed plate-glass windows because of the fact that similar windows on either side of the cracked window did not break.

CONCLUSIONS

Measurements of the shock-wave noise pressures during flight tests of fighter-type airplanes in the Mach number range between 1.13 and 1.4 and at altitudes from 25,000 to 45,000 feet indicate the following conclusions:

1. Good agreement was obtained between measured and calculated values of the pressure rise across the shock wave for locations near the flight track. There is a tendency for the theory to overestimate the pressures at locations remote from the track and to underestimate the pressures for conditions of high tailwinds at altitude.

2. The measured values of ground-reflection factor were found to average about 1.8 for a sandy ground surface and a hard plywood surface.

3. Two booms were detected in all cases by the recording instruments, the time interval ranging from 0.121 to 0.220 seconds. In general, the observers also reported two booms although one boom was reported in some cases.

4. In cases where measured ground pressures exceeded values of about 1 lb/sq ft for a steeply rising wave shape, most observers considered the noise objectionable and likened it to close-by thunder. There is an indication that the wave shape may be as important as the pressure magnitude with regard to observer reaction.

5. Cracking of a large plate-glass store window was correlated in time with the overhead passage of a fighter-type airplane at an altitude of 25,000 feet.

Langley Research Center,
    National Aeronautics and Space Administration,
        Langley Field, Va., June 26, 1959.

REFERENCES

1. DuMond, Jesse W. M., Cohen, E. Richard, Panofsky, W. K. H., and Deeds, Edward: A Determination of the Wave Forms and Laws of Propagation and Dissipation of Ballistic Shock Waves. Jour. Acous. Soc. of America, vol. 18, no. 1, July 1946, pp. 97-118.

2. Whitham, G. B.: The Behaviour of Supersonic Flow Past a Body of Revolution, Far From the Axis. Proc. Roy. Soc. (London), ser. A, vol. 201, no. 1064, Mar. 7, 1950, pp. 89-109.

3. Randall, D. G.: Methods for Estimating Distributions and Intensities for Sonic Bangs. Tech. Note No. Aero 2524, British R.A.E., Aug. 1957.

4. Mullens, Marshall E.: A Flight Test Investigation of the Sonic Boom. AFFTC-TN-56-20, Air Res. and Dev. Command, U.S. Air Force, May 1956.

5. Daum, Fred L., and Smith, Norman: Experimental Investigation of the Shock Wave Pressure Characteristics Related to the Sonic Boom. WADC-TN-55-203, U.S. Air Force, Aug. 1955.

6. Carlson, Harry W.: A Wind-Tunnel Investigation of Some Aspects of the Supersonic Boom. Aero/Space Eng., vol. 18, no. 7, July 1959, pp. 38-39, 52.

7. Von Gierke, Henning E.: Aircraft Noise Sources. Handbook of Noise Control, ch. 33, Cyril M. Harris, ed., McGraw-Hill Book Co., 1957, pp. 33-1 - 33-65.

8. Maglieri, Domenic J., and Carlson, Harry W.: The Shock-Wave Noise Problem of Supersonic Aircraft in Steady Flight. NASA MEMO 3-4-59L, 1959.

9. Anon.: Standard Atmosphere - Tables and Data for Altitudes to 65,800 Feet. NACA Rep. 1235, 1955. (Supersedes NACA TN 3182.)

10. Busemann, Adolf: The Relation Between Minimizing Drag and Noise at Supersonic Speeds. Proc. Conf. on High-Speed Aeronautics, Antonio Ferri, Nicholas J. Hoff, and Paul A. Libby, eds., Polytechnic Inst. of Brooklyn, c.1955, pp. 133-144.

TABLE I.- MEASURED GROUND SHOCK-NOISE PEAK OVERPRESSURES

Flight	Test airplane	Altitude, ft	Airplane Mach number	Measuring station	Lateral distance from flight path to station, miles	Δp_0, lb/sq ft	Δt, sec
1	1	35,000	1.40	A	3.7	0.99	0.123
				B	10.5	.65	.142
				C	14.2	----	-----
2	1	35,000	1.23	A	13.8	----	-----
				B	7.3	----	-----
				C	3.5	----	-----
3	1	25,000	1.22	A	3.5	1.75	0.136
				B	10.3	.02	.220
				C	13.8	----	-----
4	1	45,000	1.15	A	2.9	----	-----
				B	9.7	----	-----
				C	13.1	----	-----
5	1	40,000	1.31	A	3.5	1.38	0.121
6	1	45,000	1.28	A	2.1	1.08	0.126
7	2	35,000	1.13	A	2.1	0.91	0.132

TABLE II.- COMPARISON OF MEASURED AND

CALCULATED TIME INTERVALS

Flight	Station	V, ft/sec	Δt_{meas}, sec	Δt_{calc}, sec (eq. (3))
1	A	1,391	0.123	0.133
	B	1,391	.142	.155
3	A	1,244	0.136	0.140
	B	1,244	.220	.167
5	A	1,340	0.121	0.142
6	A	1,324	0.126	0.145
7	A	1,125	0.132	0.140

TABLE III.- OBSERVATIONS AND REACTIONS

Flight	Station	Δp_o, lb/sq ft	Δt, sec	Comments		
				Number of booms	Summary judgment	Remarks
1	A	0.99	0.123	1 or 2	Bothersome	Sounded like close thunder or blast set off in area
	B	.65	.142	2	Tolerable	Sounded like thunder, no visible reaction from people in nearby field
	C	----	-----	------	Not objectionable	Rumbling like distant storm, no visible reaction from people in vicinity
2	C	----	-----	1	Not objectionable	Sounded like distant explosion, no visible reaction from people in vicinity
3	A	1.75	0.136	2	Very objectionable	Like very close thunder, reported damage to plate-glass window and grocery items shaken from shelves
	B	.02	.220	-----	Not objectionable	Rumbling sounded like distant thunder, no visible reaction from people in nearby field
5	A	1.38	0.121	2	Objectionable	Sounded like close thunder, strong complaint received by telephone, this flight only few minutes ahead of 7
6	A	1.08	0.126	2	Tolerable	Sounded like close thunder or gun blasts, formation of ducks scattered
7	A	0.91	0.132	2	Objectionable	Observers thought more severe than 5

········· Radar track
— — Estimated flight track

CHESAPEAKE BAY

ATLANTIC OCEAN

Wallops Station

N

0   10,000 20,000
Scale, feet
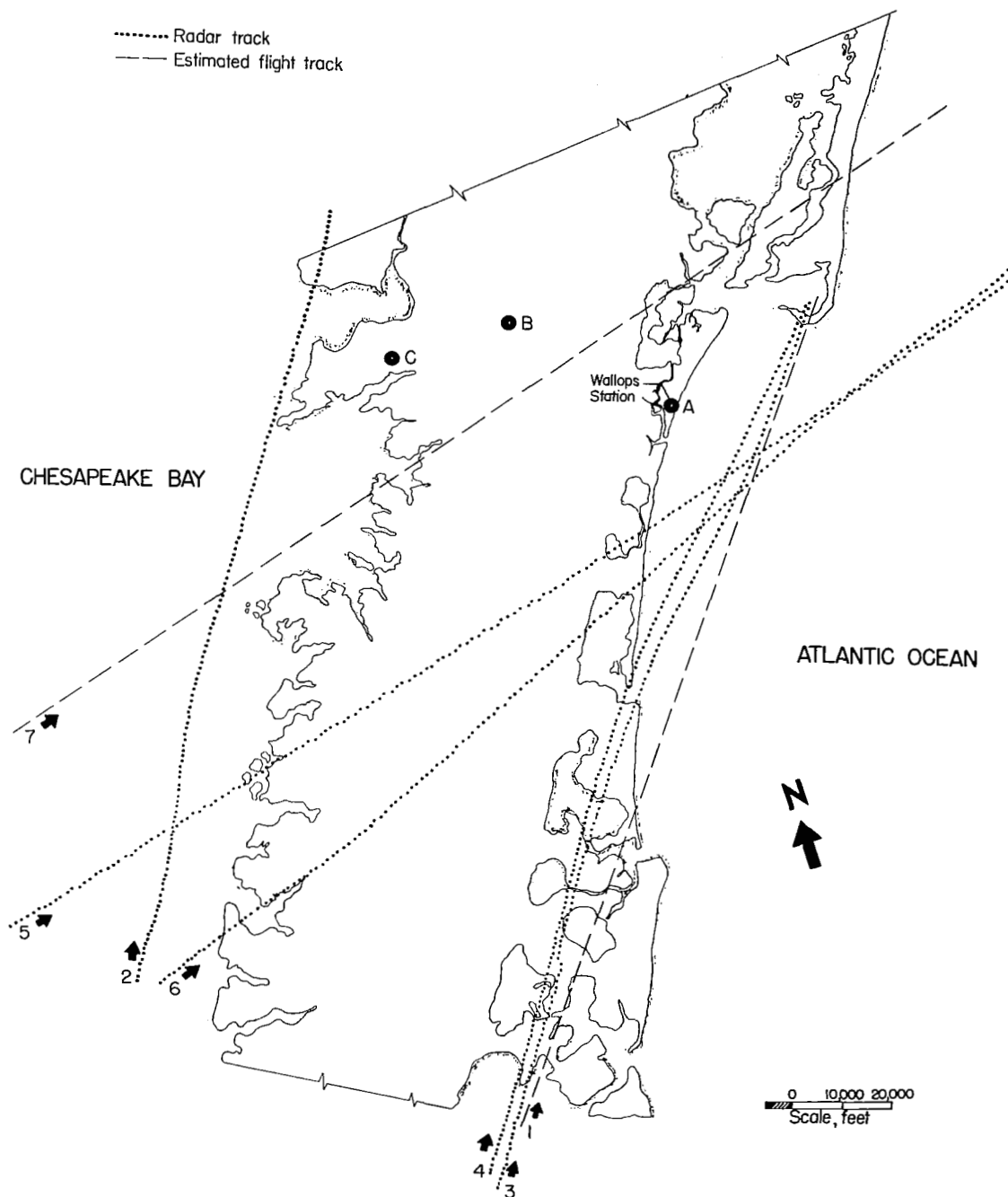
Figure 1.- Map of test area showing measuring stations and superposed
radar tracks for test flights.
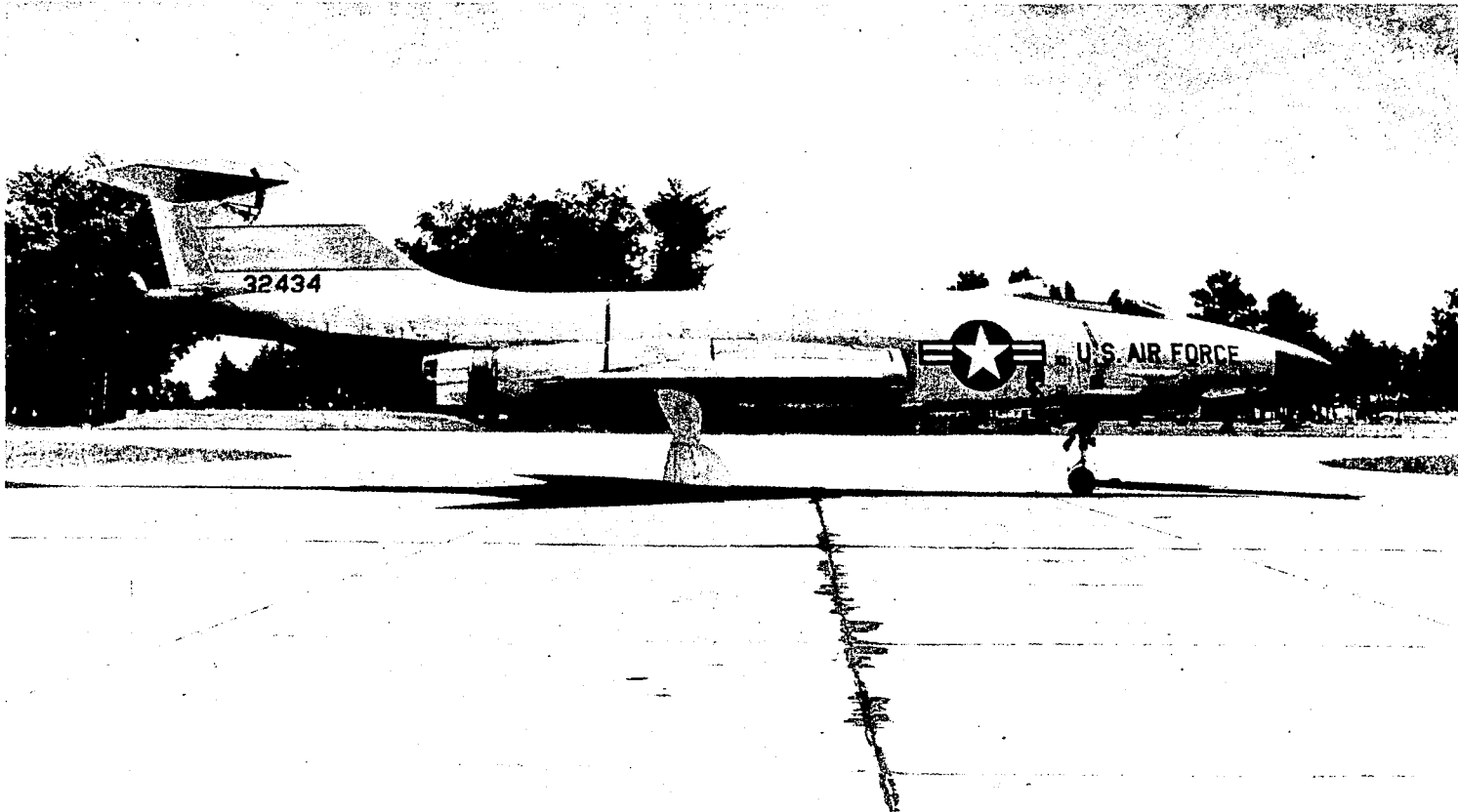
(a) Airplane 1.   L-95153.1

Figure 2.- Test airplanes.

(b) Airplane 2.   L-58-1842.1

Figure 2.- Concluded.

22
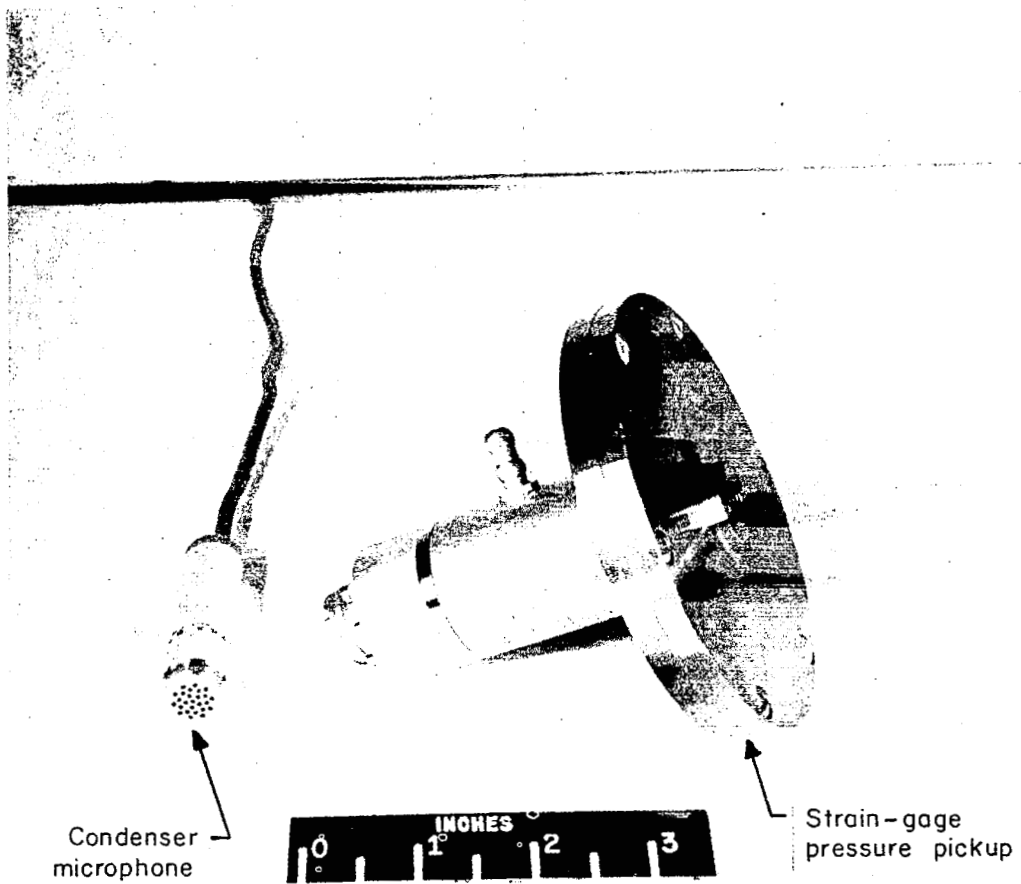
L-59-1414.1

Figure 3.- Condenser microphone and resistance-type strain-gage pressure cell.

Approximate
flight
direction

5 ½'

$\frac{3}{16}$" steel plate

3' 8'

$\frac{3}{4}$" plywood

4' 3'

N

Microphone

Mast

30'

Microphone

5'

Microphone

Pressure gage

Ground level
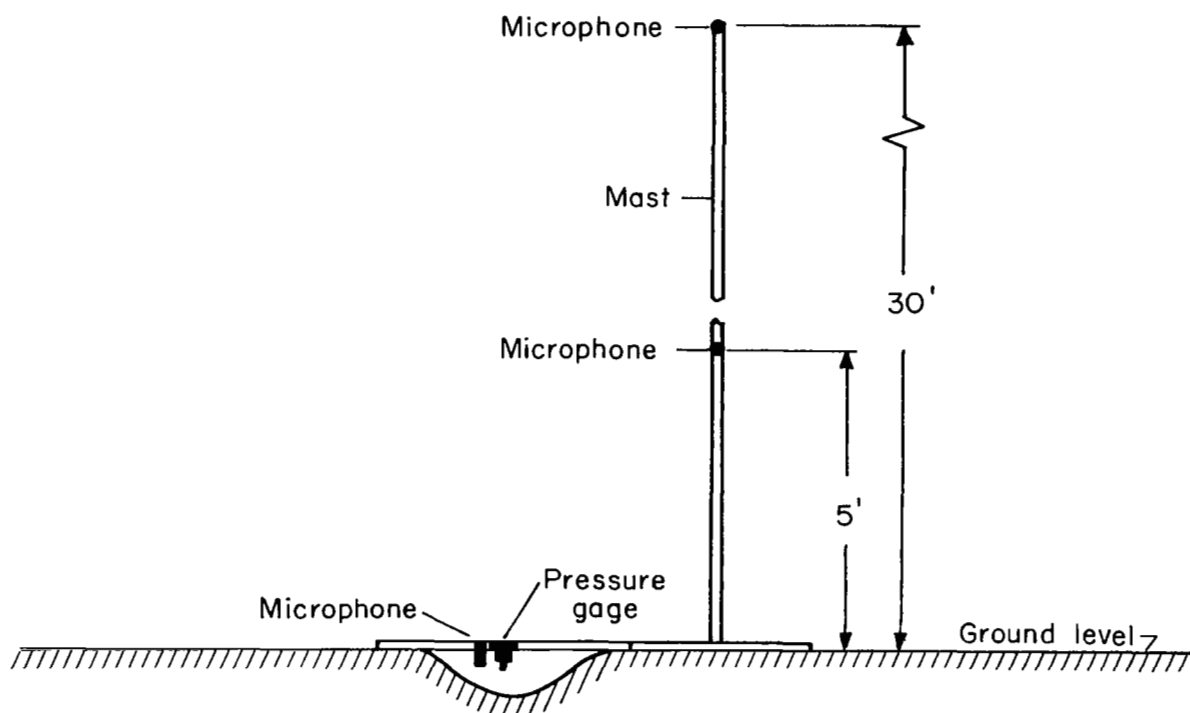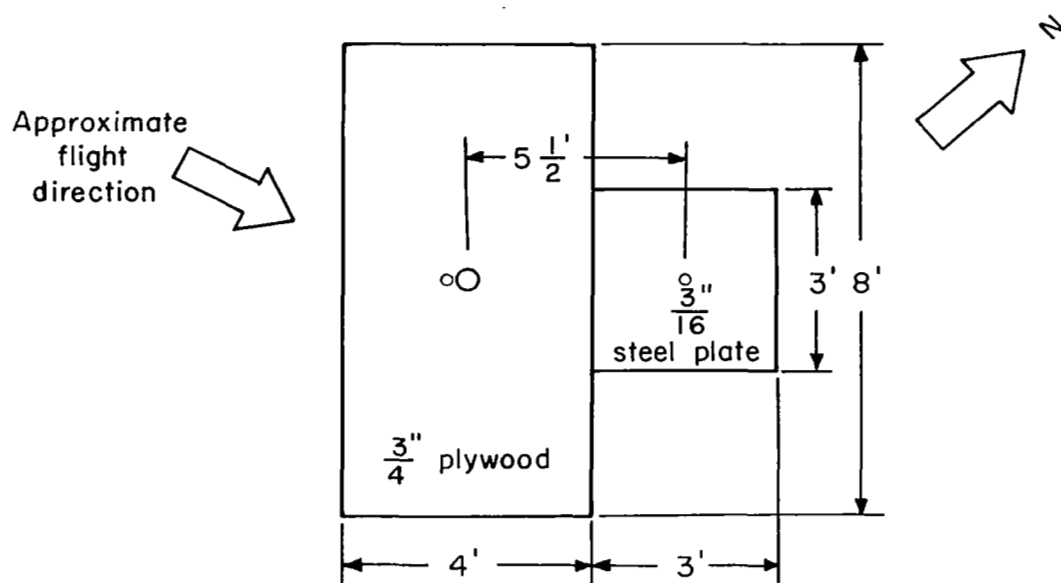
Figure 4.- Test setup used for measuring ground, free-air, and reflected wave pressures.

24
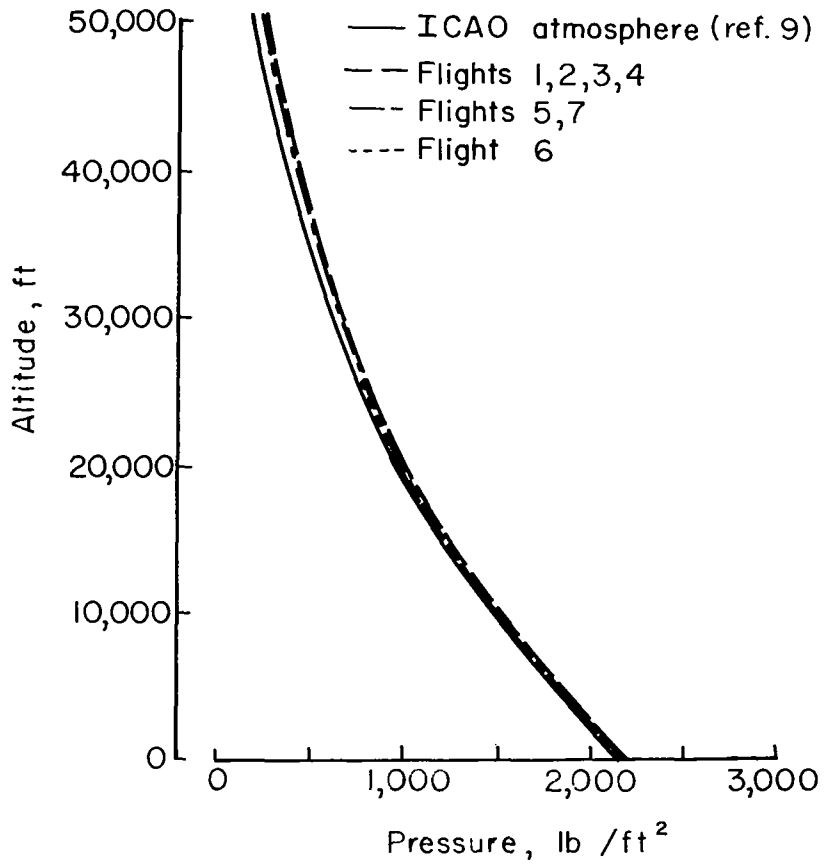
Figure 5.- Results from atmospheric soundings taken during test flights.
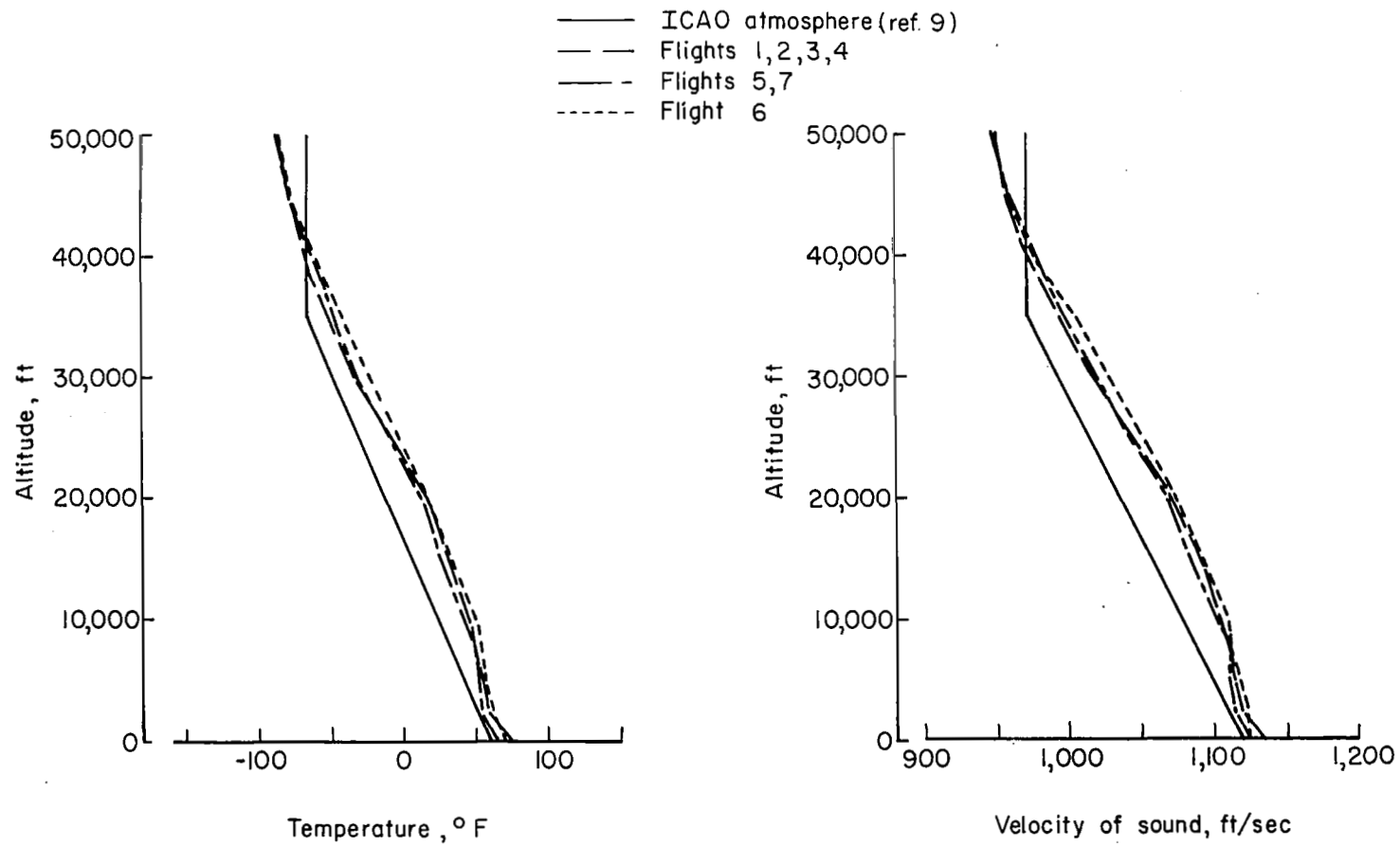
Figure 5.- Concluded.
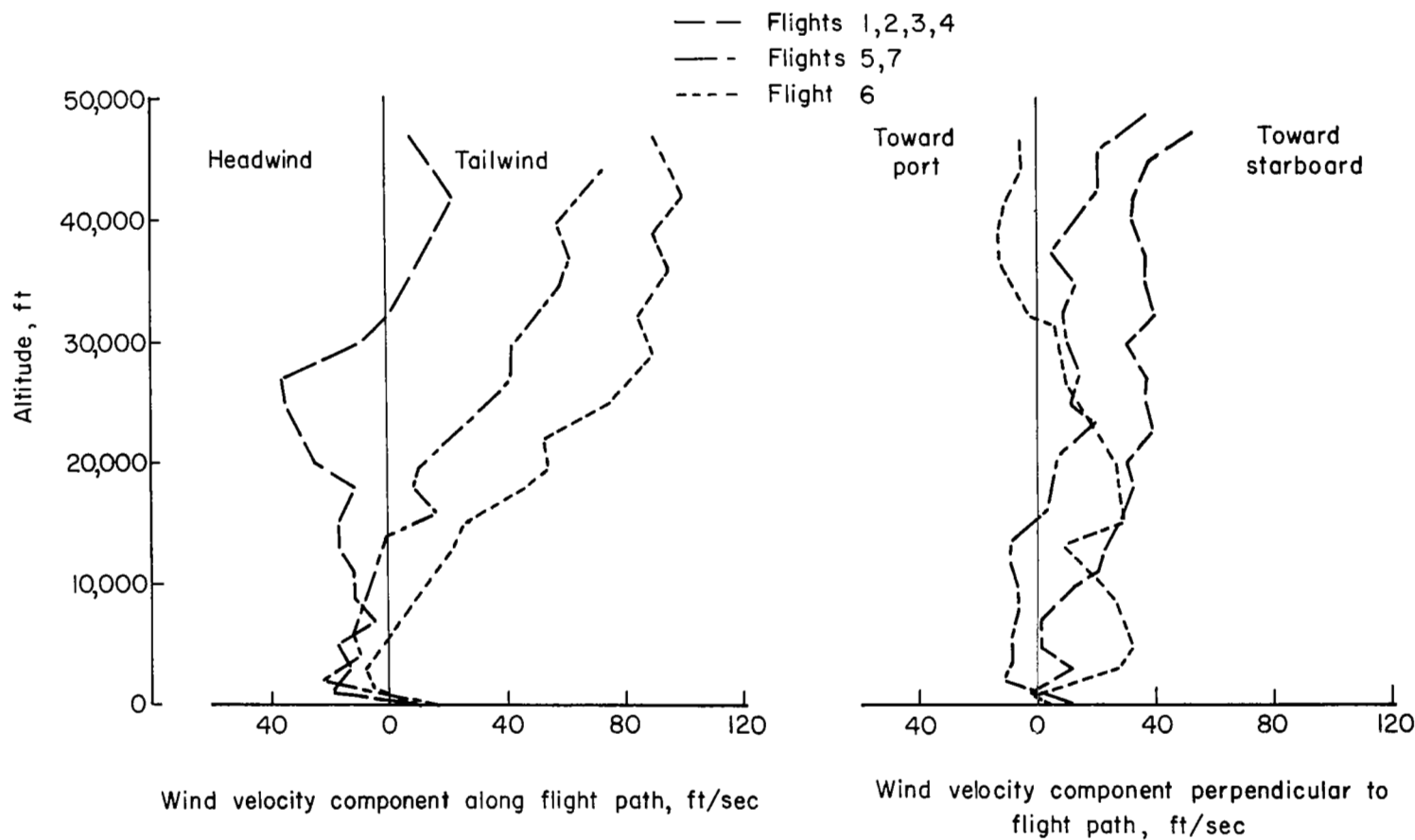
Figure 6.- Wind data obtained from atmospheric soundings taken during test flights.
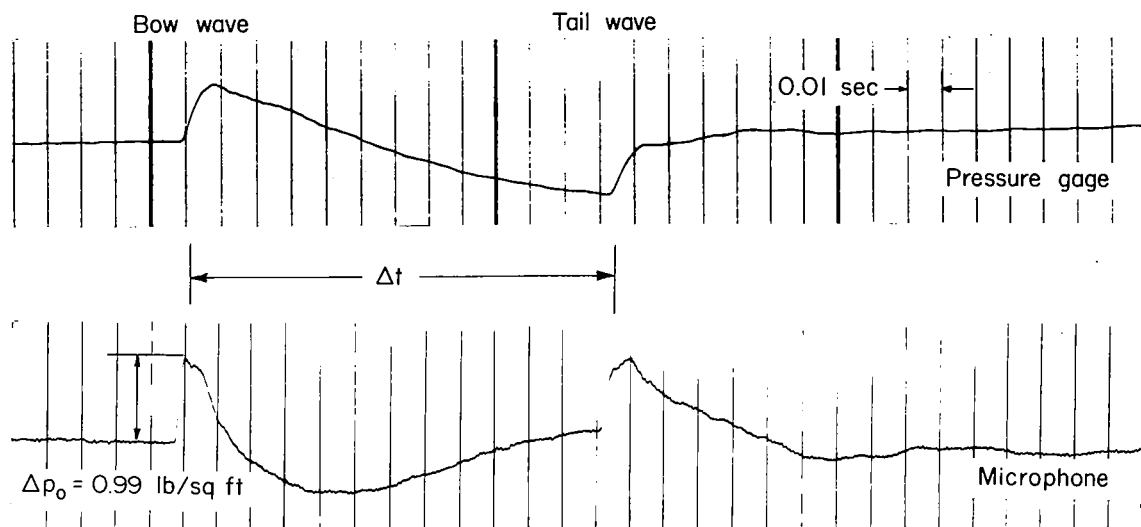
(a) Station A (3.7 miles laterally from flight track).
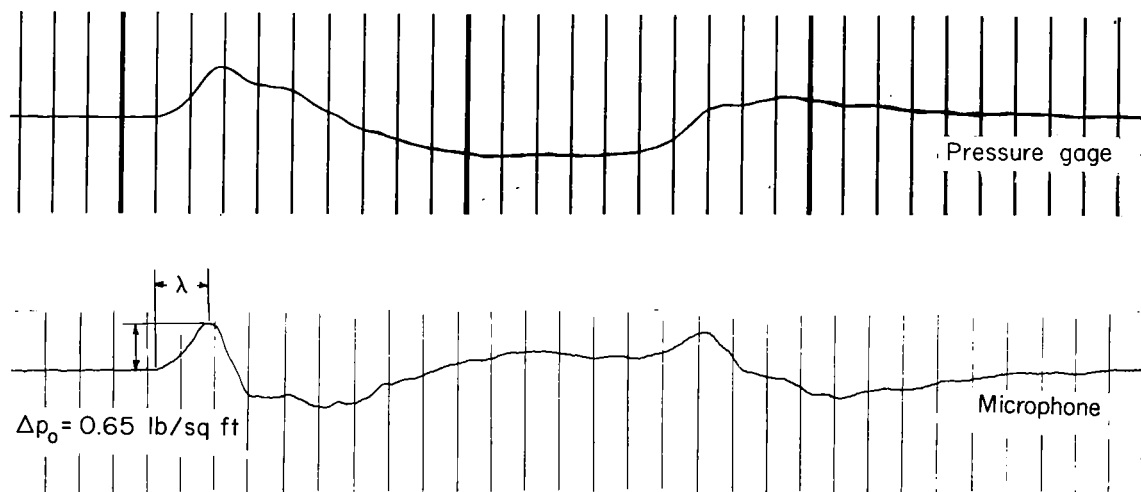
(b) Station B (10.5 miles laterally from flight track).

Figure 7.- Time histories of ground shock-noise pressures for flight 1 as obtained from pressure gages and microphones located at stations A and B.
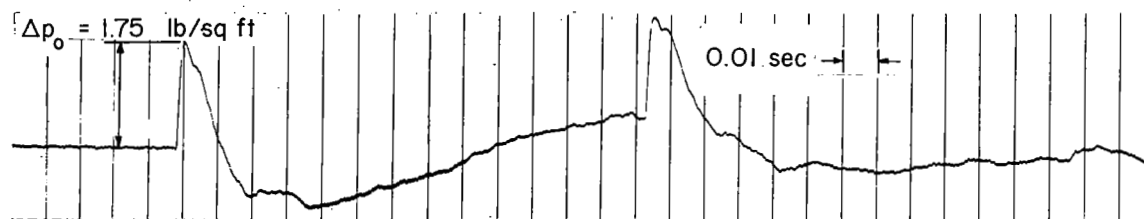
(a) Altitude, 25,000 feet; flight 3.
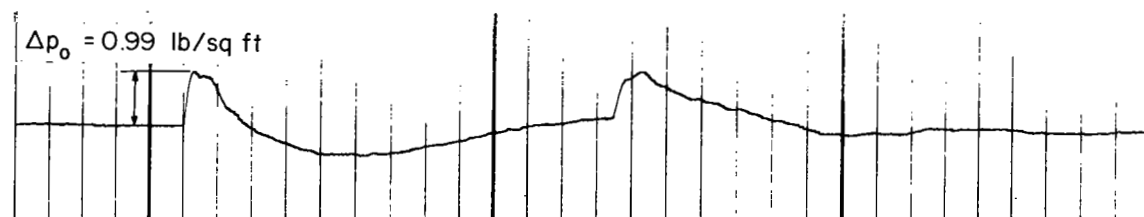
(b) Altitude, 35,000 feet; flight 1.
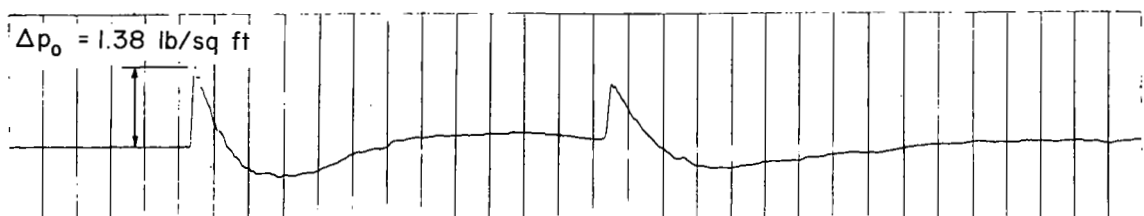
(c) Altitude, 40,000 feet; flight 5.

(d) Altitude, 45,000 feet; flight 6.

Figure 8.- Time histories of ground shock-noise pressure from flights at four altitudes as obtained with microphone located at station A.

$\Delta p_o = 1.38$ lb/sq ft

0.01 sec
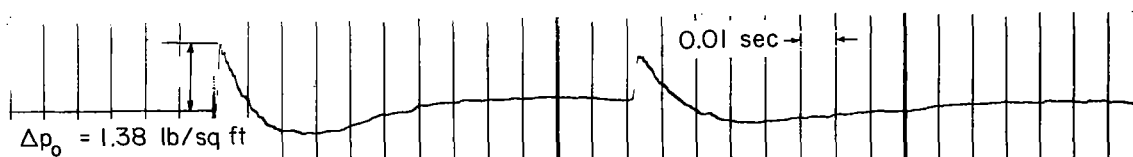
(a) Microphone at ground level.

$\Delta p_f = 0.78$ lb/sq ft
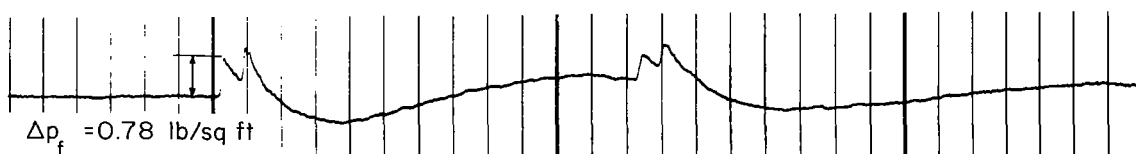
(b) Microphone at 5-foot elevation.

$\Delta p_r = 0.545$ lb/sq ft

$\Delta p_f = 0.78$ lb/sq ft
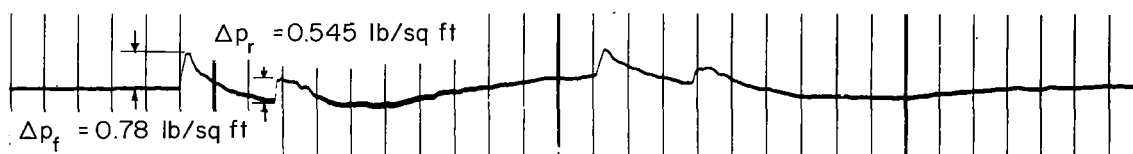
(c) Microphone at 30-foot elevation.

Figure 9.- Time histories of shock-noise pressures for flight 5 as obtained from microphones located at various heights at station A.
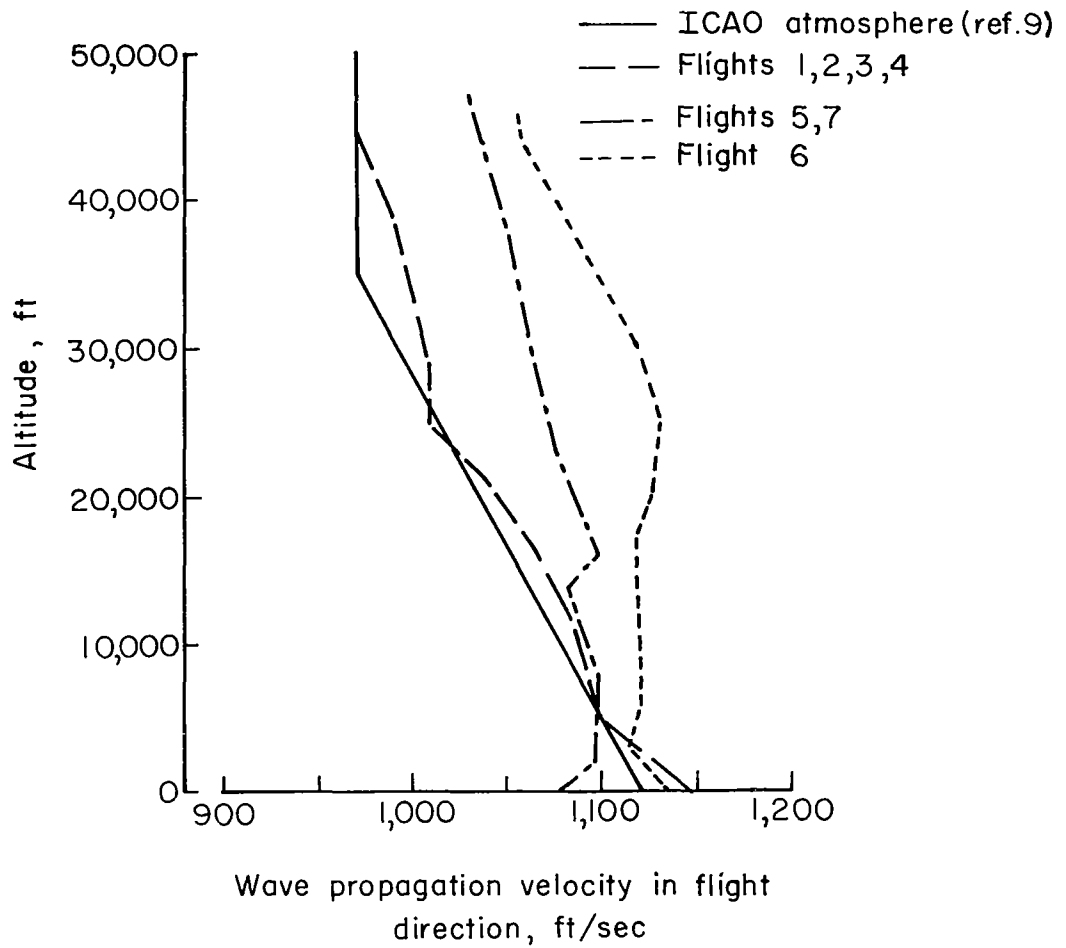
Figure 10.- Variation of wave propagation velocity with altitude.
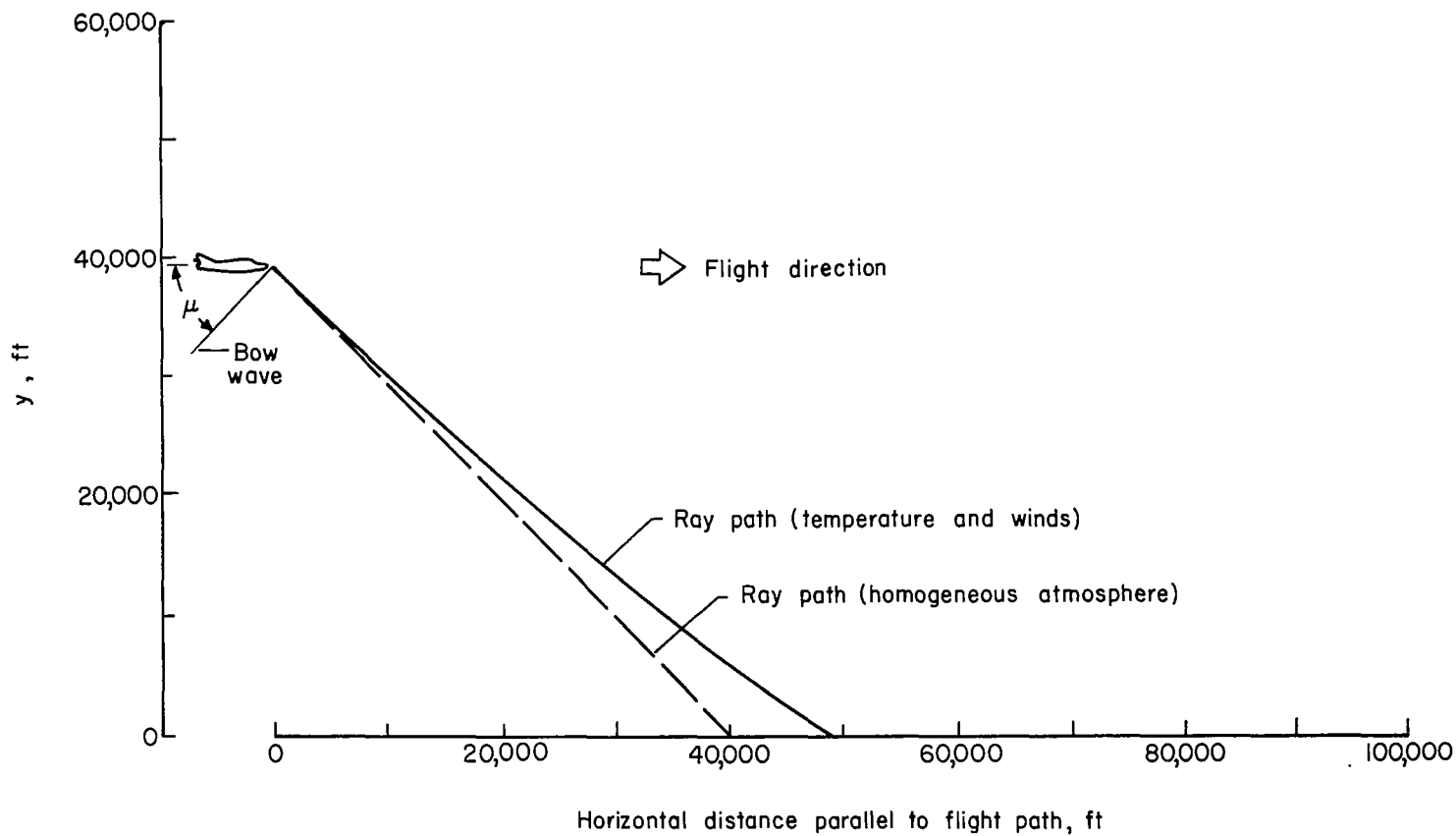
(a) Flight 1; M = 1.4.

Figure 11.- Calculated ray paths of bow-wave propagation.
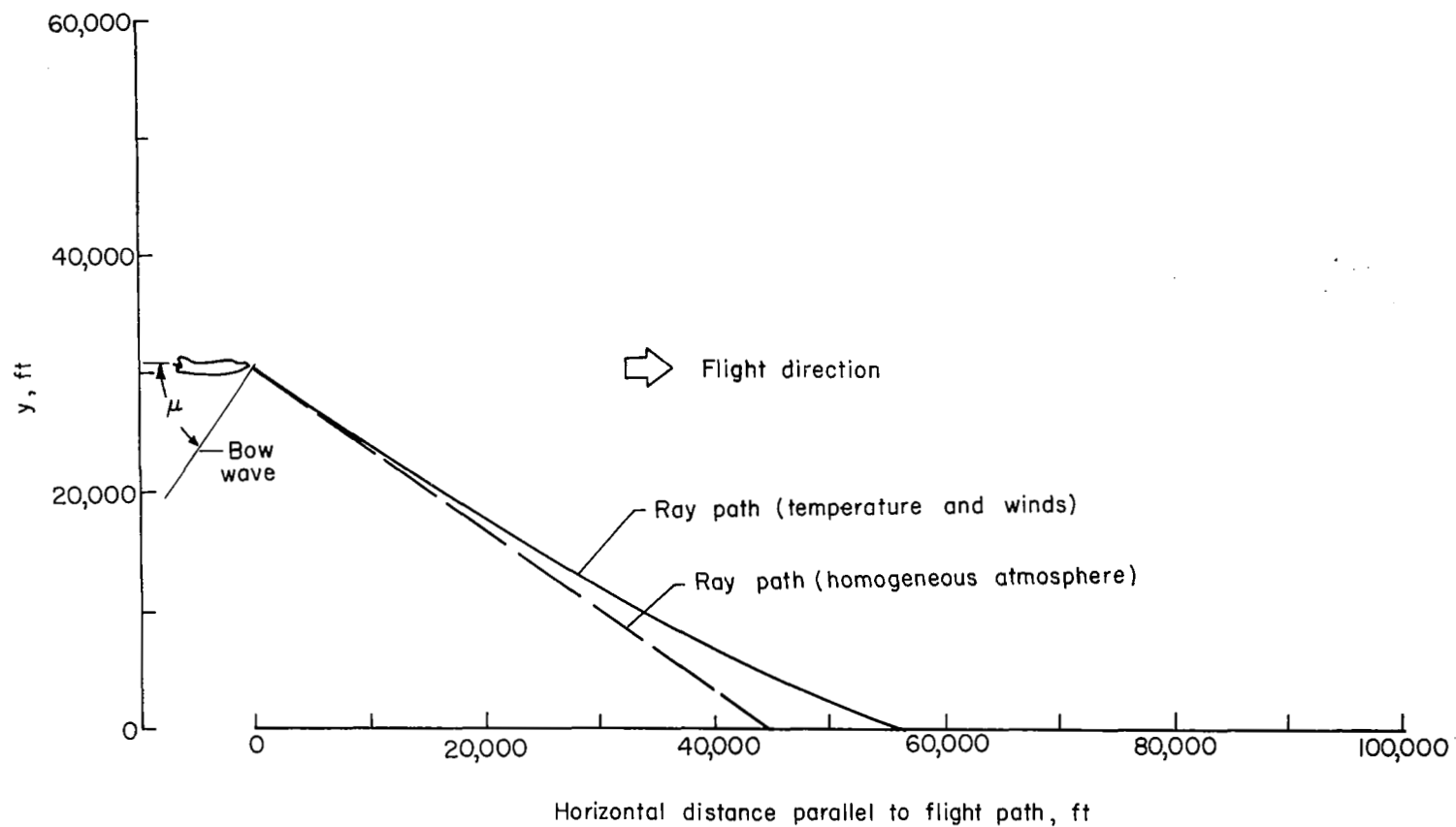
(b) Flight 3; M = 1.22.

Figure 11.- Continued.
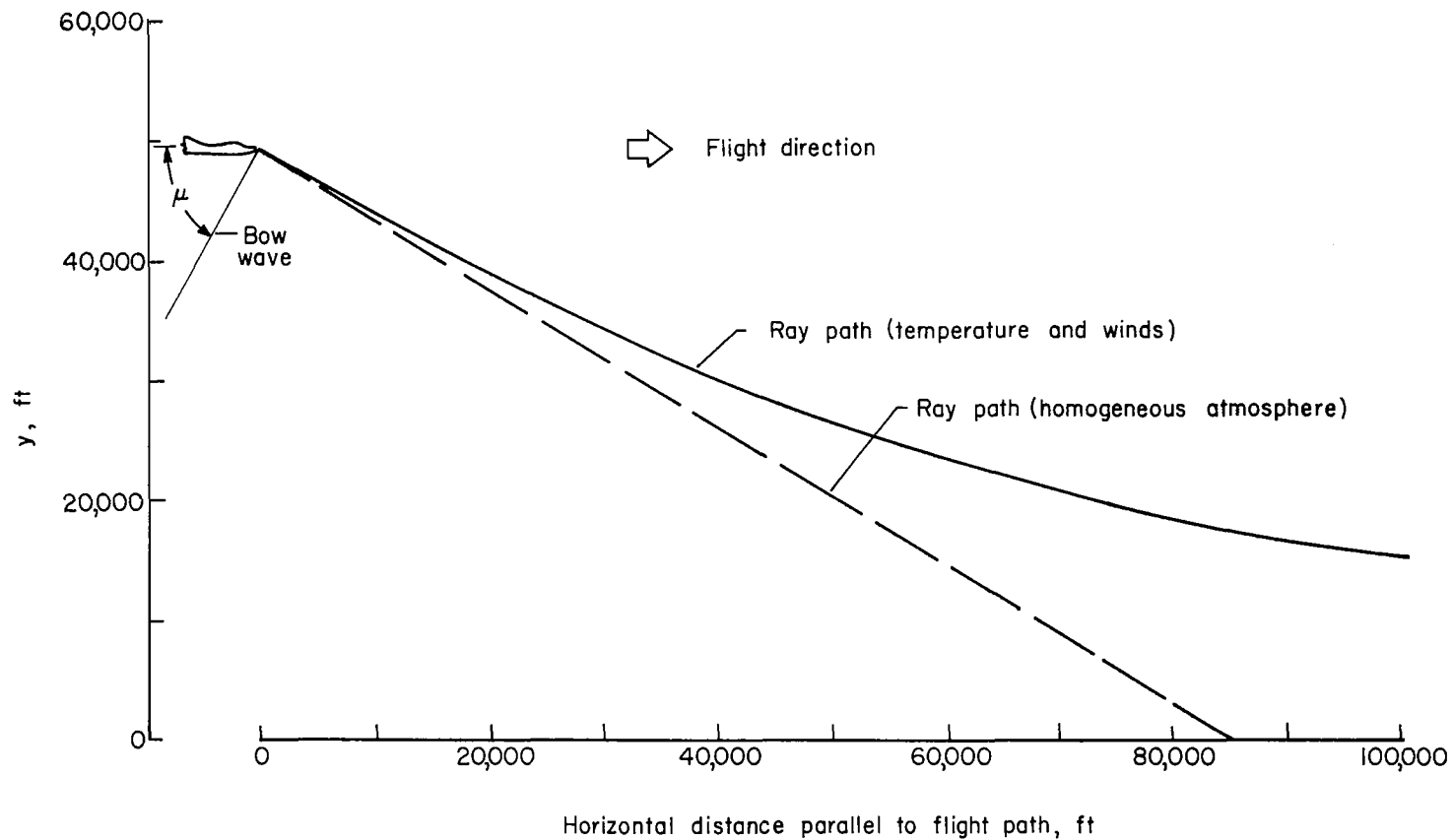
(c) Flight 4; M = 1.15.

Figure 11.- Continued.
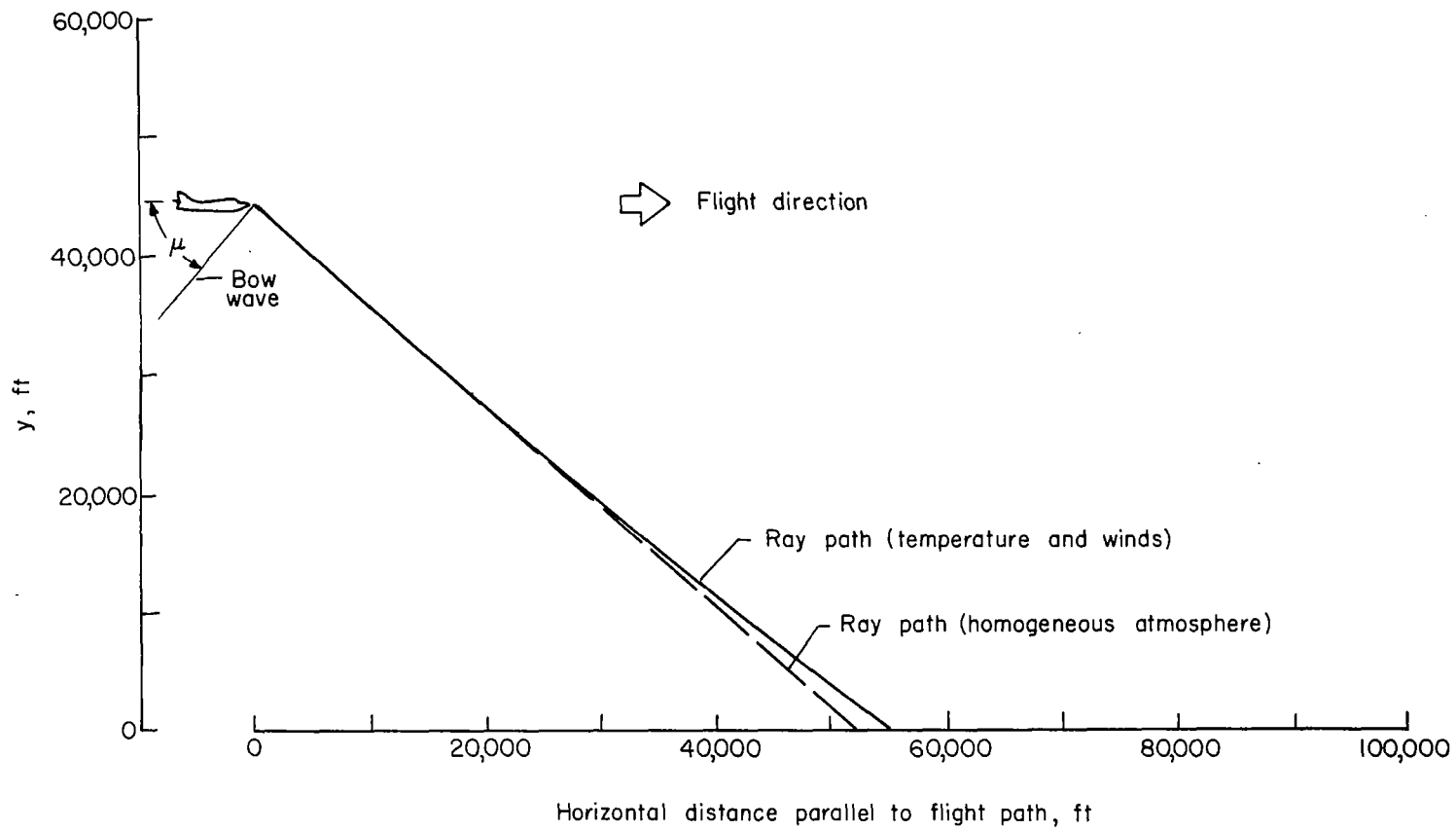
(d) Flight 5; M = 1.31.

Figure 11.- Continued.
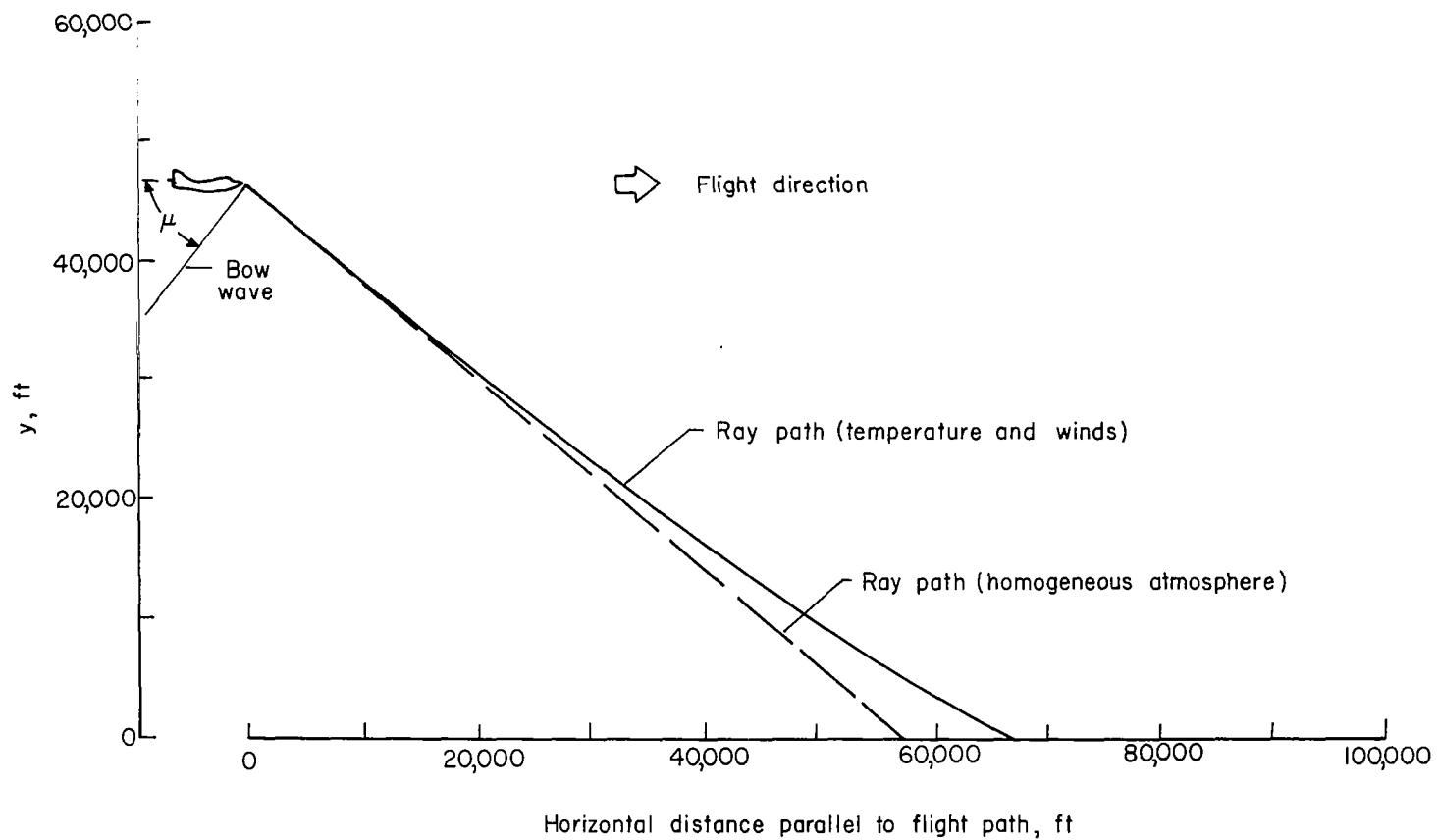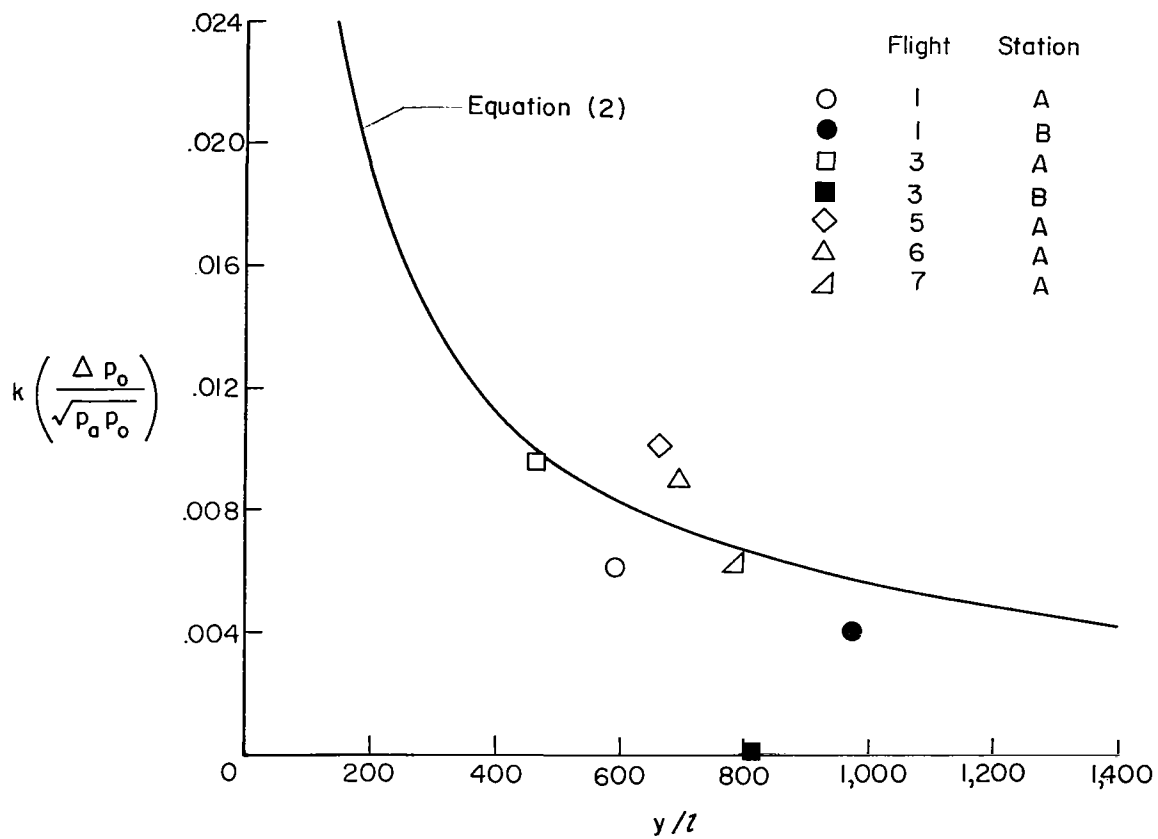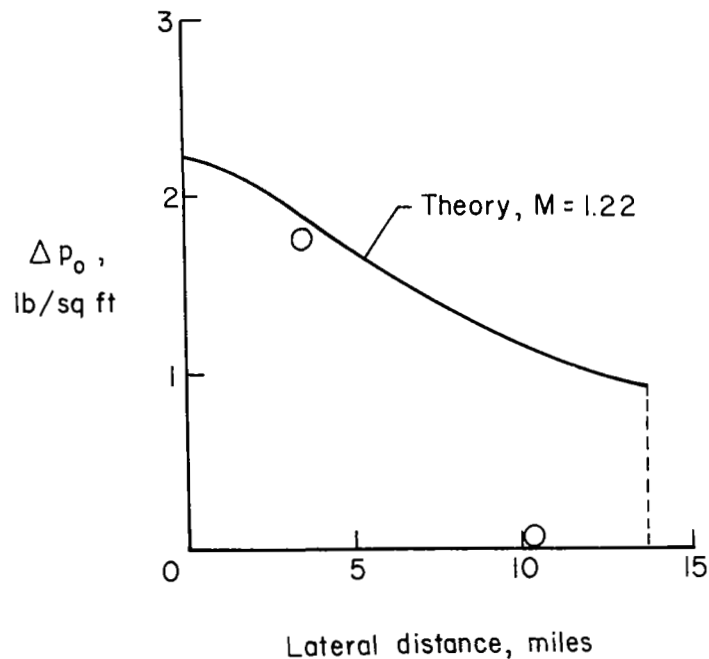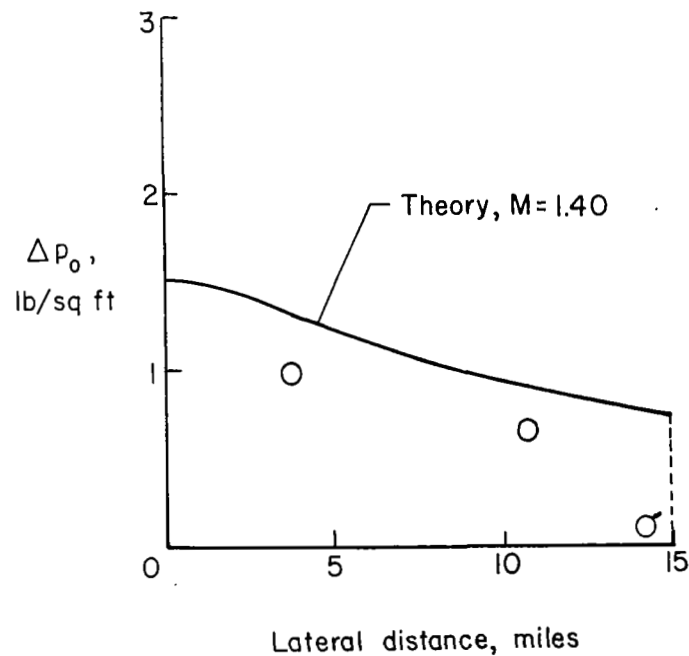
(e) Flight 6; M = 1.28.

Figure 11.- Concluded.

Figure 12.- Comparison of calculated and measured ground pressures.

(a) Altitude, 25,000 feet.

(b) Altitude, 35,000 feet.

Figure 13.- Comparison of calculated and measured ground pressures for test airplane 1. (Flagged symbol indicates estimated value.)
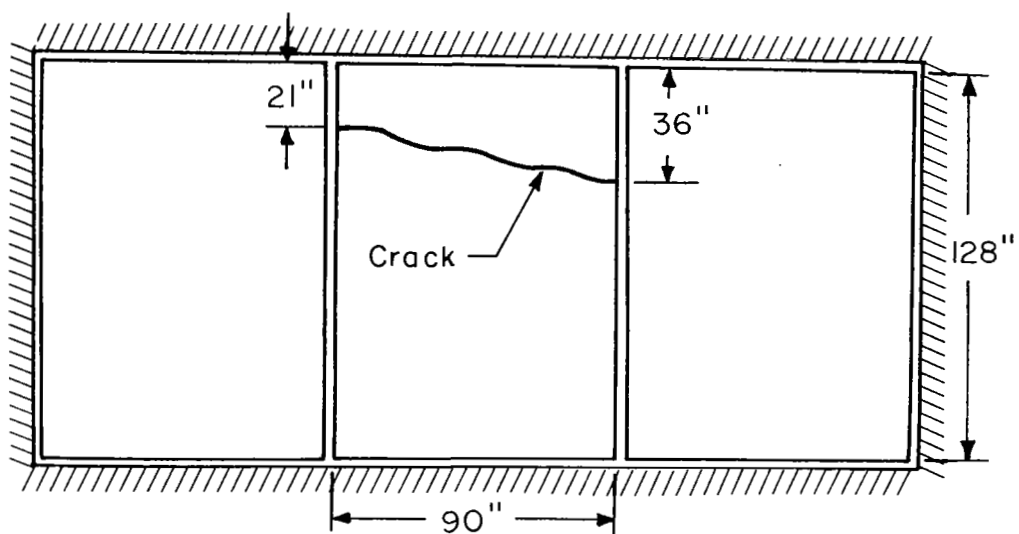
Figure 14.- Schematic diagram showing nature of damage to 1/4-inch-thick plate-glass store window.